ACADEMIC PRESS

Available online at www.sciencedirect.com
SCIENCE DIRECT®

Journal of Catalysis 214 (2003) 46–52

JOURNAL OF CATALYSIS

www.elsevier.com/locate/jcat

Effect of surface reconstruction of $TiO_2(001)$ single crystal on the photoreaction of acetic acid

J.N. Wilson and H. Idriss *

Department of Chemistry, The University of Auckland, Private Bag 92019, Auckland, New Zealand

Received 17 May 2002; revised 18 October 2002; accepted 21 October 2002

Abstract

Unlike dark catalytic reactions, mainly dependent on the last-layer atomic arrangement, photoreactions on semiconductor surfaces depend necessarily on the bulk properties of the solid materials. Decoupling of the effect of surface and bulk structures can be obtained by allowing for surface reconstruction. The photocatalytic reaction of acetic acid on the two different reconstructed surfaces of $TiO_2(001)$ single crystal (the {011}- and the {114}-faceted surfaces) under ultrahigh vacuum conditions was conducted. The reaction products (ethane, methane, water and CO_2: photo-Kolbe reaction) were found to be similar on both reconstructed surfaces. Quantitative analyses show, however, a large difference in reactivity. The low temperature annealed surface, the {011}-faceted surface, was found far more reactive than the high temperature annealed surface, the {114}-faceted surface. The quantum yield of the reaction of acetic acid was found equal to 0.05 and 0.02 for the {011}- and {114}-faceted surfaces, respectively. This large difference in reactivity is solely due to the collective changes of the electric field created by changing the last-layer atomic arrangement. From the catalytic reaction, the depletion layer width (W) and barrier height (V) for both surfaces could be computed. The depletion layer widths (*as well as the barrier heights*) were found equal to 18.2 and 6.6 nm (0.18 and 0.023 V) for the {011}- and {114}-faceted surfaces, respectively.

Keywords: Titanium oxide; Photochemistry; Photoreaction; Depletion layer; Acetic acid; Barrier height

1. Introduction

Considerable studies have been devoted to understanding the surfaces of well-defined rutile titanium oxides in the past two decades [1–3] because of their use in several important technologies ranging from catalysis [4] and solar cell devices [5] to biomaterials [6]. Although some sporadic works have considered the photoreaction of simple organic molecules over TiO_2 single crystals only very few examples have focused on the effect of surface structure on the photocatalytic process [7,8]. This work addresses the effect of changing the surface structure of rutile $TiO_2(001)$ single crystal (used as a prototype surface) on the photoreaction of acetic acid (as an example of an organic molecule) under steady-state conditions under UHV and we do find that the low temperature reconstructed surface (the {011} faceted surface) is considerably more active than the high temperature reconstructed one (the {114} faceted surface) [1].

Several detailed studies have been conducted concerning the photoreactions of acetic acid over TiO_2 powders. The products and intermediates observed have been investigated using several techniques including infrared (IR) [9], mass spectroscopy (MS) [10], electron spin resonance (ESR) [11], and photoelectrochemical studies [12]. The main reaction has been termed photo-Kolbe with the products being ethane, methane, and carbon dioxide. The two reaction pathways identified are as follows:

$$CH_3COOH_{(ads)} \rightarrow CO_{2(g)} + CH_{4(g)}, \quad (1)$$

$$2CH_3COOH_{(ads)} + \mathbf{O}_{(lattice)} \rightarrow 2CO_{2(g)} + CH_3CH_{3(g)} + H_2\mathbf{O}_{(ads)}, \quad (2)$$

Acetic acid when adsorbed on the surface of $TiO_2(001)$ and (110) single crystals is dissociated into acetate species (CH_3COO^-) and bound to titanium atoms, and the proton forms (^-OH) with surface oxygen atoms. Over $TiO_2(110)$ single crystal the carboxylate is bound in a bidentate configuration, with a saturation coverage of 0.5 [13–16]. These species have been well studied via X-ray photoelectron spectroscopy (XPS) [17], ultraviolet photoelectron spec-

* Corresponding author.
E-mail address: h.idriss@auckland.ac.nz (H. Idriss).

0021-9517/03/$ – see front matter
doi:10.1016/S0021-9517(02)00172-0

troscopy (UPS) [18], temperature programmed desorption (TPD) [17], electron stimulated desorption ion angular distributions (ESDIAD) [14], and scanning tunneling microscopy (STM) [15]. Under dark conditions, during TPD these species desorb as acetic acid and water with the additional products being carbon monoxide, ketene, and carbon dioxide (see TPD in the results section). The reactions of carboxylic acids were also studied under UV light by several authors [19,20]. Reaction (1) is proposed to occur via a methyl radical ($\cdot CH_3$) abstracting the dissociated hydrogen producing methane and CO_2, while reaction (2), is proposed to occur via two ($\cdot CH_3$) molecules forming ethane, CO_2, and H_2O. These species have been thoroughly investigated, with perhaps the most compelling evidence coming form a study involving monodeuterated acetic acid (CH_3COOD) [10,20]. The authors found no incorporation of deuterium into ethane but D_2O and CH_3D did form in high yield, indicating the simple reaction scheme is indeed correct. Perhaps the most important difference is that the latter reaction (2) requires lattice oxygen: addition of oxygen into the gas phase increased the production of ethane [reaction (2)] [10]. It was suggested that this oxygen replenishes the lattice, which becomes deficient/reduced (TiO_{2-x}) due to the formation of water.

Working on a single crystal surface has the advantage of knowing to a reasonable accuracy the atomic arrangement and surface stoichiometry. The ideal surface of $TiO_2(001)$ single crystal contains Ti atoms fourfold coordinated to oxygen atoms and this makes them unstable (high surface energy). It facets to two thermodynamically stable structures: the {011}- and the {114}-faceted structures. These structures are obtained by annealing in vacuum at 700–750 and 900–950 K, respectively [1,4]. The first structure {011} contains Ti atoms in a fivefold coordination environment while the second one {114} contains Ti atoms in four, five, and six coordination in equal proportions (maintaining an overall coordination of Ti atoms of 5) (Fig. 1). In this work the photoreaction of acetic acid with the two surface structures of $TiO_2(001)$ single crystal is studied under flow conditions in UHV. The effect of both acetic acid and oxygen partial pressures on the reaction products is monitored and discussed.

2. Experimental

All experiments were conducted in an ultrahigh vacuum (UHV) chamber described in detail previously [21]. In brief the UHV chamber is pumped with an ion, turbo molecular and titanium sublimation pump to a base pressure of $\sim 2 \times 10^{-10}$ torr and is equipped with a quadrupole mass spectrometer (up to 300 amu), with pyrex shroud, ion sputter gun, heating stage (x, y, r motion feed through), ion gauge, and two dosing lines with dosing needle positioned a few millimeters away from the crystal face. The single crystal of $TiO_2(001)$ is prepared with sputter and anneal cycles, typically Ar^+ pressure 1×10^{-5} torr, 5-kV beam voltage, 25-mA

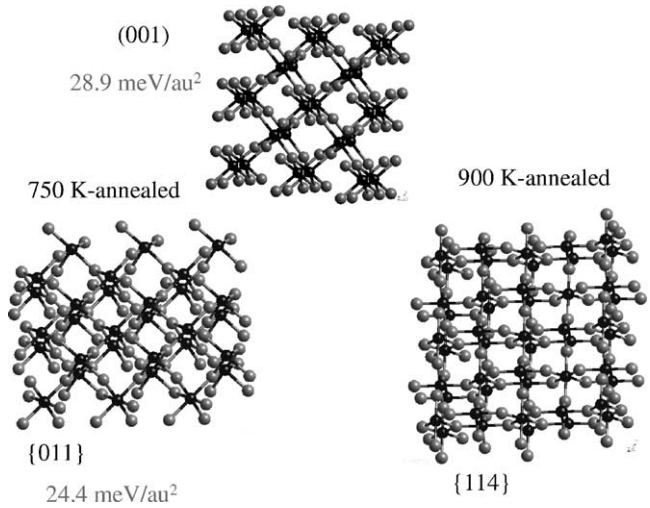

Fig. 1. Surface structures of $TiO_2(001)$, 750 K annealed, {011}-faceted, and 900 K annealed, {114}-faceted (relaxed surface energies are given for the (001) and (011) surfaces in meV/au^2; there are no data for the {114}-faceted surface). Gray, and black balls, oxygen and titanium, respectively.

emission current, followed by several "flashes" at either 750 or 900 K under oxygen pressure, 1×10^{-6} torr, for 10-min intervals. The $TiO_2(001)$ single crystal is positioned in such a way that the flux of acetic acid is reflected into the mass spectrometer probe and that the focused "beam" of UV light, Spectroline Model SB-100P/F high intensity lamp (365 nm), is illuminating only the surface. Once a steady flow of acid onto the crystal surface has been achieved and a sufficient baseline recorded a shutter is opened allowing the UV to strike the surface. After a time period (~ 5 min) the shutter is closed and this process is repeated at different pressures of acetic acid. In a separate set of experiments a steady state of acetic acid is maintained and oxygen pressure is varied through a separate dosing line. Acetic acid is purified on the dosing line by a repeated freeze-pump-thaw process and the oxygen gas put through a series of dry ice traps.

In order to calculate the reaction rate for the photodecomposition of acetic acid on both surfaces the flow rate of acetic acid was required. The basic equation of pressure and flow rate for a vacuum pump is

$$P = \frac{Q}{S} + P', \tag{3}$$

where P is the pressure of chamber (torr) during the reaction; S the intrinsic pumping speed (mL/s), P' the ultimate pressure of the pump (taken as 2×10^{-10} torr), and Q is the flow rate (in units of torr mL/s). Dividing the flow rate by kT yields the molecular flow rate. The flow rate had values between (2×10^{-7} and 3×10^{-4} torr mL/s). The contact time with the single crystal was then estimated by dividing the amount of acetic acid (expressed in molecules) by the molecular flow rate (molecules/(molecules/s) $= \tau$); Fig. 2 shows more details.

The flux of the UV photons reaching the crystal was determined by actinometry via titration of acidified (1 mol/L

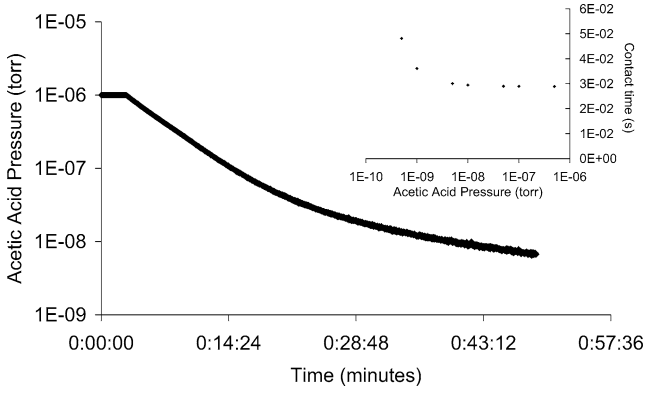

Fig. 2. Pumping speed of the chamber, Inset: contact time as a function of acetic acid pressure.

HNO_3) uranyl nitrate (0.02 mol/L) and oxalic acid (0.05 mol/L) solution with permanganate (0.025 mol/L) and was found equal to ca. $5 \times 10^{15}\ h\nu\ \mathrm{cm}^{-2}\,\mathrm{s}^{-1}$.

In order to calculate the quantum yield, $\eta =$ (rate/flux) ($\sum$ molecules converted/cm^2 s)/(photons/cm^2 s), an estimation of the total molecules reacted was computed from the total amount of carbon-containing molecules (the surface of the single crystal is 1 cm^2). Combining Eqs. (1) and (2) gives 1 molecule of ethane, one molecule of methane, and three molecules of CO_2 formed per three molecules of acetic acid.

3. Results and discussion

3.1. Temperature-programmed desorption (dark studies)

The dark reaction of acetic acid was first considered as a reference guide since a similar study by other workers has been conducted [17]. On the {011}-faceted surface acetic acid was mainly dehydrated to ketene and water (at 570 K). Some decomposition to CO, CO_2 at 610 K also occurred. The {114}-faceted surface of TiO_2(001) is obtained by annealing at 900 K and above for a prolonged time. One of the main characteristics of this surface is the presence of Ti atoms in a four coordination environment (in other words contains two coordinative unsaturation, Fig. 1). Numerous examples have shown the production of ketones from carboxylic acids on this surface. The formation of ketones (such as acetone from acetic acid [17] and divinylketone from acrylic acid [22]) was attributed to a concerted reaction whereby two adsorbed carboxylate species on one unsaturated Ti center (Ti_{4c}, where c stands for coordination number) react together yielding one molecule of ketone and one molecule of CO_2 leaving one oxygen atom on the surface:

$$\mathrm{CH_3COO}\mathbf{Ti_{4c}}\mathrm{OOCCH_3} \rightarrow \mathrm{CH_3COCH_3} + \mathrm{CO_2} + \mathbf{Ti_{5c}{-}O}. \quad (4)$$

The extent of reaction (and consequently formation of the {114}-faceted surface) was tracked, in the case of acetic acid reactivity, by the ratio product/reactant (acetone (m/z 58)/acetic acid (m/z 60)) and is shown in Fig. 3. While a 5-min annealed surface shows only traces of acetone, annealing for 50 min has resulted in large formations of acetone. The product yield of acetic acid-TPD on both surfaces is shown in Table 1. Thus the presence (or absence) of acetone from acetic acid is a clear indication of the presence (or absence) of the surface reconstruction from the {011}-faceted (absence of acetone) to the {114}-faceted surface (presence of acetone).

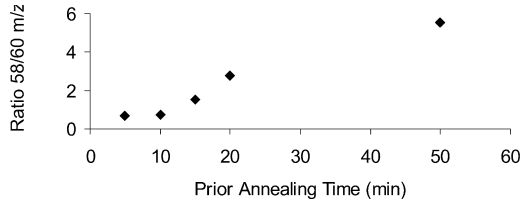

Fig. 3. Acetone production from acetic acid (TPD) as a function of annealing time at 900 K.

3.2. Steady-state reactions under UV

In the absence of UV no other products but acetic acid were observed at the reaction temperature (320 K). This is expected since as shown in Ref. [17] and Table 1 carboxylic acids do not react (to other products) below 450–500 K on TiO_2 single crystal surfaces. Steady state with UV illumination was conducted at several acetic acid pressures (as monitored by its m/z 60 signal) between 5×10^{-10} and 6×10^{-7} torr at ca. 320 K. Fig. 4 shows a representative data conducted on the {011}-faceted surface with acetic acid pressure equal to 2.5×10^{-9} torr in the presence of background oxygen molecules (noncalibrated m/z 32 signal ca. 5×10^{-10} torr). Three products, carbon dioxide, methane, and ethane, are clearly seen as a jump in the line spectra from the initial baseline value. Both CO_2 (m/z 44) and methane (m/z 16) reach a steady state of formation quickly as the UV shutter is opened. In contrast the ethane (m/z 30) formation reaches a high value initially and drops to a steady value after a short time (< 20 s). This latter observation is further investigated below. The photoreaction of acetic acid appears sensitive to surface structure. Fig. 5

Table 1
Product yield % of acetic acid over TiO_2(001)-{011}- and TiO_2(001)-{114}-faceted surfaces

Molecule	Peak temperature K	Yield (%) {011}	Yield (%) {114}
Acetic acid	400	0.94	0.23
	570	4.52	0.93
CO_2	570	3.02	6.80
CO	570	9.56	38.09
H_2O	400	0.83	1.57
	610	5.27	2.19
Ketene	570	75.87	43.75
Acetone	550	–	6.44

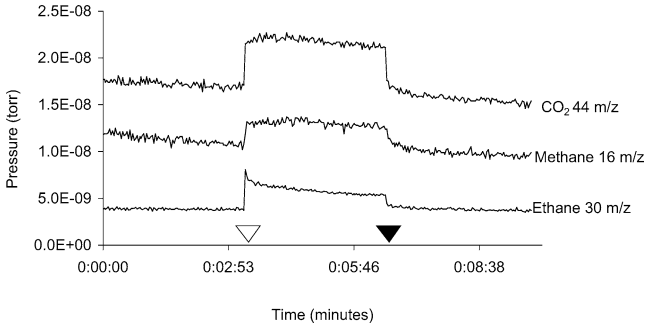

Fig. 4. Steady-state acetic acid pressure 2.5×10^{-9} torr on the {011}-faceted TiO_2 (001) surface. Open and closed triangle, UV light on and off, respectively.

shows the comparison between the activity of both surfaces (the {011} and the {114}) for ethane (the most important product) formation from acetic acid in the same pressure domain. The {011}-faceted surface is more active than the {114}-faceted surface.

The formation of ethane requires lattice oxygen to be consumed [reaction (2)] and as the outermost layer is depleted the formation of ethane is reduced. To test this explanation oxygen is introduced into the gas phase, via a secondary dosing line. This is shown in Fig. 6. Clearly no decrease in ethane signal is observed. Moreover, there

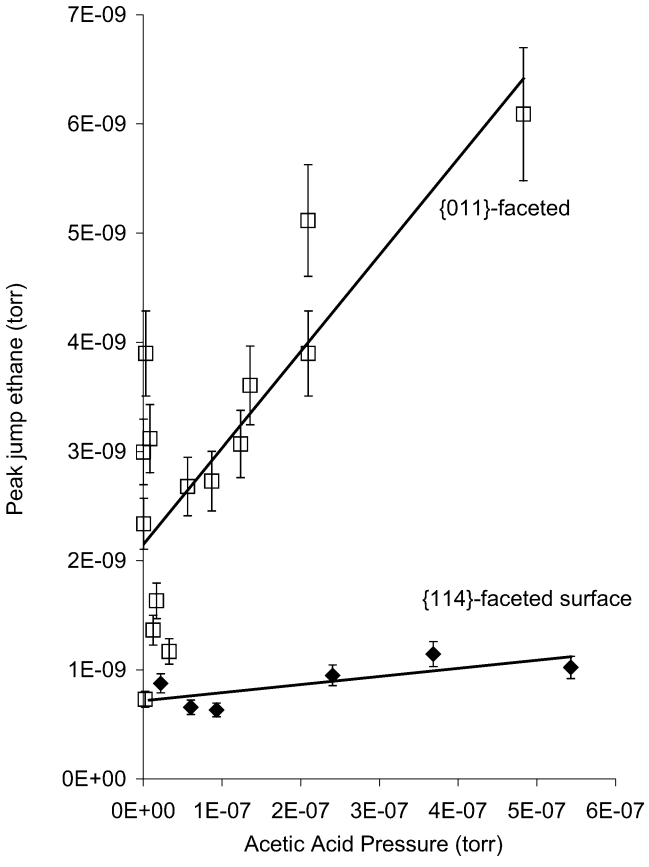

Fig. 5. Ethane (m/z 30) production (under UV illumination) as a function of acetic acid pressure over the two TiO_2(001) single crystal surfaces.

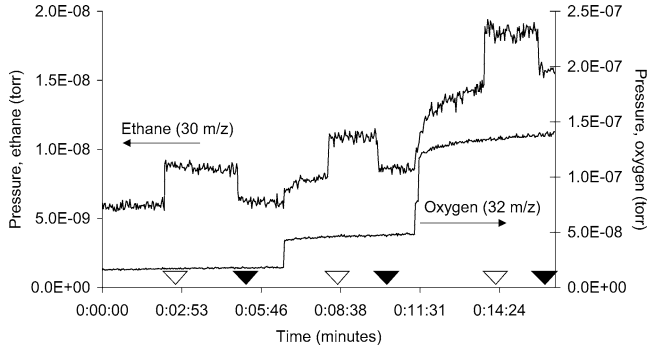

Fig. 6. Formation of ethane (m/z 30) under steady-state reaction conditions on the {011}-faceted TiO_2(001) single crystal surface at a constant acetic acid pressure 5×10^{-9} torr and increasing pressure of O_2. The rise in the m/z 30 signal under dark conditions is due to the increase of the overall chamber pressure. Open and closed triangle, UV light on and off, respectively.

is a mild increase of ethane formation with increasing O_2 partial pressure. The effect of changing O_2 partial pressures on the formation of ethane and methane from acetic acid is shown in Fig 7. While ethane signal increases (Fig. 7a) that of methane decreases (Fig. 7b). This indicates a competitive pathway between reactions (1) and (2).

4. Discussion

In electron or charge-transfer processes, between a semiconductor and an adsorbate, photogeneration of electrons and holes determines the extent of reaction. In competition with this process, electron-hole recombination takes place. The photocatalytic activity has been shown to depend on several parameters such as crystal structure [24], particle size [23,25,27,29], defects [26], and doping [28,30]. There are basically three requirements for a high catalytic activity: that the photogenerated charge carriers exist near the surface, that they have a long lifetime, and that the rate of charge transfer is large. The rate of electron-hole pair recombination affects the lifetime of the charge carriers and thus directly affects the catalytic activity. Decreasing (increasing) the band bending increases (decreases) the rate of recombination because there is less (more) driving force for electron-hole separation. It is worth reminding that for an n-type semiconductor the minority carriers (the holes) preferentially migrate to the surface because of the direction of the electric field [31]. In the following we will discuss the difference in the observed reaction rate between both surfaces from knowledge developed from light-induced charge separation theories and the effect of depletion-layer on the photoreaction of a semiconductor.

We first start with a qualitative description as outlined in Eq. (5):

$$CH_3COOH + \mathbf{Ti}\text{–}\mathbf{O} \rightarrow \mathbf{Ti}\text{–}OCOCH_3 + \mathbf{O}H. \quad (5)$$

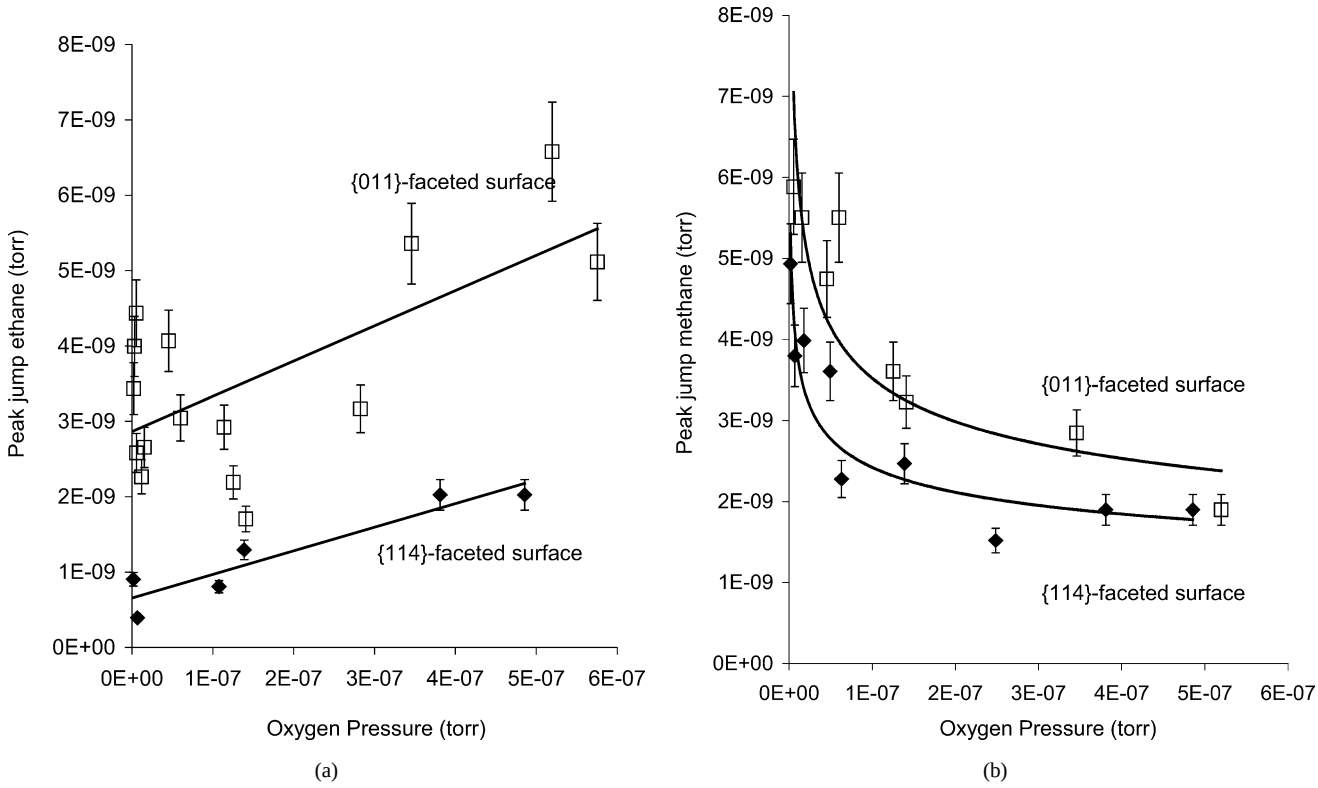

Fig. 7. (a) Ethane (m/z 30) production as a function of oxygen pressure, constant acetic acid pressure (5×10^{-9} torr). The points of the {011}-faceted TiO_2 (001) single crystal surface are more scattered because it cannot be annealed to high temperature and is thus more sensitive to surface contamination. The trend is however clear: with the exception of two points all other points are far higher than those obtained from the {114}-faceted TiO_2(001) single crystal surface. The error bars are those of mass spectrometer reading (7–8%). (b) Methane (m/z 16) production as a function of oxygen pressure, constant acetic acid pressure (5×10^{-9} torr) on the two surface reconstruction of TiO_2(001) single crystal under UV illumination.

Adsorption of an acetic acid molecule on a **Ti**–**O** center results in the formation of an acetate and a surface hydroxyl species. Upon illumination of TiO_2 (n-type semiconductor) and creation of charge carriers (h^+ and e^-: from electron transfer from the valence band to the conduction band), migration of h^+ to the surface (due to field provoked by the depletion layer) may result in a hydroxyl radical formation. Simultaneously, reactions of an electron with an acceptor center (such as O_2 to $O_2^{\cdot}$ or Ti^{4+} to Ti^{3+}) occur [32,33]. The local arrangement of these **Ti**–**O** atoms (see Fig. 1) does not appear to influence the reaction pathway since the products of both surfaces were found the same (in sharp contradiction with dark reactions). This indicates that, unlike the dark reaction, the photocatalytic reaction products are not selectively influenced by the surface structure. However, there is a considerable difference in the reaction activity (see Fig. 7). This difference is most likely related to the intrinsic physical properties of each surface due to a different atomic arrangement giving a specific but collective electronic property for each surface. Computation of the quantum yield, η, for each surface may help in probing some of these properties. η was found equal to 0.05 and 0.02 for the {011}- and {114}-faceted surfaces, respectively.

4.1. Estimation of the depletion width from the quantum yield of the reaction

The quantum yield of a photoreaction is related to the depletion layer width (W). In the case of TiO_2 it is a layer depleted of the majority carriers (electrons) and the distance between the Fermi level and the conduction-band minimum is increased. In other words, the band will be bent upward. Absorption of photons will generate electron-hole pairs in the depletion layer and their generation rate is in general constant through the layer (provided its width is sufficiently small compared to the penetration depth of the incident light). Eq. (6) relates the quantum yield to the width of the depletion layer [31],

$$\eta = \frac{L + W}{1/\alpha + L}, \tag{6}$$

with α the reciprocal absorption length $= 2.6 \times 10^4$ cm^{-1} at 320 nm [31] and L, the minority carrier diffusion length,

$$L = \sqrt{D\tau}, \tag{7}$$

D is the diffusion coefficient and τ is the mean carrier lifetime. The mean carrier life-time has been approximated by random walk analysis by other workers [34]: the average transit time from the interior of the particle to the surface is

expressed by

$$\tau = \frac{r_o^2}{\pi^2 D} = \frac{L_{Deb}^2}{\pi^2 D}. \quad (8)$$

In the presence of a depletion layer, the Debye length, L_{Deb} (the maximum distance between an electron and a hole formed upon photoirradiation) replaces r_o as long as the size of the material is large (not of quantum size). The intrinsic Debye length, L_{Deb} is expressed as [33]

$$L_{Deb}^2 = \frac{\varepsilon \varepsilon_o k_B T}{2e^2 n_i}, \quad (9)$$

ε for static dielectric constant, ε_o for vacuum permittivity, and the other symbols have their usual meaning. ε along the (001) direction for TiO_2 is equal to 170 [35], since it is only the last layer that is reconstructed then ε for both structures can be reasonably considered the same. Moreover, the bulk to surface diffusion of both electron and holes is probably very similar for both surfaces. The number of charge carriers, n_i, has been computed by several workers and several values were given (10^{23}–10^{25} m^{-3}). The calculations reported here are for $n_i = 10^{25}/m^3$ for TiO_2. The computed value for L_{Deb} was found equal to ca. 3.5 nm. τ is estimated equal to 0.6 ps and L (mean carrier diffusion length) was found equal to 1.1×10^{-7} cm.

From these values W was found equal to 18.2 and 6.6 nm for the {011}- and {114}-faceted surfaces, respectively. This result explains in physical terms the reason behind the difference in reactivity of the two surfaces. The {011}-faceted surface is more active than the {114}-faceted surface because the photogenerated electrons and holes have a larger space and so their recombination rate will be smaller.

From the above data one can also obtain an estimation of the barrier height (in V) of the surface band banding, see Fig. 8, resulting from the depletion layer following [33]

$$e|V| = \frac{e^2}{2\varepsilon\varepsilon_o} n_i W^2. \quad (10)$$

This was found equal to 0.18 and 0.023 V for the {011}- and {114}-faceted surfaces of TiO_2(001) single crystal, respectively.

4.2. An estimation of the upper quantum yield of the reaction of acetic acid over rutile TiO_2 surfaces

It is instructive given these results to estimate the maximum quantum yield expected with the above-quoted numbers. Assuming that a barrier height of 1.0 eV can be reached (it is about 0.5 eV for a typical semiconductor [33]) a quantum yield of ca. 0.25 caused by a depletion layer of 50 nm can be obtained. This is probably the highest level expected for this reaction over a rutile TiO_2 surface.

4.3. The role of gas-phase oxygen

Results of this work on single crystal surfaces, together with those of other works [10,19] on polycrystalline surfaces, indicate that O_2 is required for the photo-Kolbe reaction to occur in a catalytic way on the surface of TiO_2. Inspection of Eq. (5) shows that O_2 is needed to regenerate the surface oxygen vacancies formed due to water formation (as a side reaction). However there is more into O_2 molecules then a regeneration of surface oxygen vacancies. As shown in Fig. 8, O_2 may combine with electrons transferred to the conduction band and form $O_2^{\cdot}$. Recent results on TiO_2(110) single crystal indicate that this pathway might actually contribute in the photoreaction in addition to (or instead of) the traditionally accepted route of OH radicals [26]. Another recent XPS work has shown that the presence of O_2 molecules in the gas phase is essential for the decomposition of acetate species on TiO_2(110) single crystal [36].

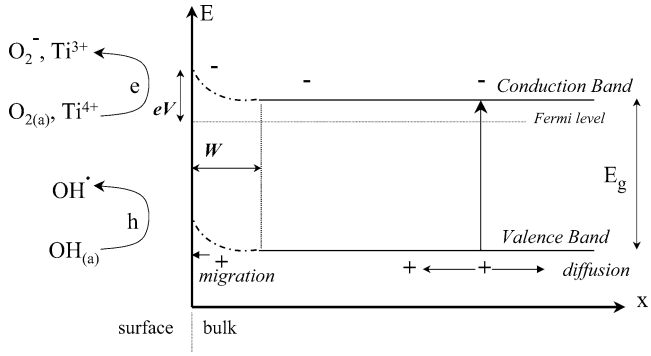

Fig. 8. A schematic representation of the space charge region of n-TiO_2. E_g, band gap; W, depletion width, eV, barrier height; x is distance into the material from the surface and E is the energy scale. Also shown the reaction of surface hydroxyls with holes formed at the valence band and surface Ti (and adsorbed oxygen molecules) with electrons at the conduction band.

5. Conclusions

By changing the outer surface structure of TiO_2(001) single crystal one can decouple the effect of bulk structure from that of the surface and this is particularly useful for photoreactions because of their high dependence on bulk properties. The steady-state photocatalytic decomposition of acetic acid was successfully conducted in UHV on the surfaces of TiO_2(001) single crystal. The low temperature annealed surface (the {011}-faceted surface) is far more reactive than the high temperature one (the {114}-faceted surface). Computation of the quantum yield, allowing the determination of both the depletion layer width and height, was conducted from the steady-state kinetics data (Table 2).

Table 2
The quantum yield (η), the width of the depletion layer (W) and the barrier height (V) for the two reconstructed surfaces of TiO_2(001) single crystal

	{011}-faceted	{114}-faceted
η	0.05	0.02
Width, W (nm)	18.2	6.6
Height, V	0.18	0.023

References

[1] M.A. Barteau, Chem. Rev. 96 (1996) 1413.
[2] A.L. Linsebigler, G. Lu, J.T. Yates Jr., Chem. Rev. 95 (1995) 735, and references therein.
[3] B.G. Daniels, R. Lindsay, G. Thornton, Surf. Rev. Lett. 8 (2001) 95.
[4] H. Idriss, M.A. Barteau, Adv. Catal. 45 (2000) 261.
[5] L. Patthey, H. Rensmo, P. Persson, K. Westmark, L. Vayssieres, A. Stashans, A. Petersson, P.A. Brühwiller, H. Siegbahn, S. Lunell, N. Mårtensson, J. Chem. Phys. 110 (1999) 5913.
[6] F.H. Jones, Surf. Sci. Rep. 42 (2001) 75.
[7] M. Anpo, H. Yamashita, Y. Ichihashi, S. Ehara, J. Electroanal. Chem. 396 (1995) 21.
[8] G. Lu, A. Linsebigler, J.T. Yates Jr., J. Phys. Chem. 99 (1995) 7626.
[9] L-F. Liao, C-F. Lien, J-L. Lin, Phys. Chem. Chem. Phys. 3 (2001) 3831.
[10] D.S. Muggli, J.L. Falconer, J. Catal. 187 (1999) 230.
[11] Y. Nosaka, K. Koenuma, K. Ushida, A. Kira, Langmuir 12 (1996) 736.
[12] B. Kraeutler, A.J. Bard, J. Am. Chem. Soc. 2239 (1978).
[13] I.D. Cocks, Q. Guo, R. Patel, E.M. Williams, E. Roman, J.L. de Segovia, Surf. Sci. 377–379 (1997) 135.
[14] Q. Guo, I. Cocks, E.M. Williams, J. Chem. Phys. 106 (1997) 2924.
[15] Q. Guo, E.M. Williams, Surf. Sci. 433–435 (1999) 322.
[16] B.E. Hayden, A. King, M.A. Newton, J. Phys. Chem. B 103 (1999) 203.
[17] K.S. Kim, M.A. Barteau, J. Catal. 125 (1990) 353.
[18] S.H. Kim, P.C. Stair, E. Weitz, Langmuir 14 (1998) 4156.
[19] D.F. Ollis, C-Y. Hsiao, L. Budiman, C-L. Lee, J. Catal. 88 (1984) 89.
[20] D.S. Muggli, J.L. Falconer, J. Catal. 191 (1999) 318.
[21] J.N. Wilson, D.J. Titheridge, H. Idriss, J. Vac. Sci. Technol. A 18 (4) (2000) 1887.
[22] D. Titheridge, M.A. Barteau, H. Idriss, Langmuir 17 (2001) 2120.
[23] T. Reztova, C.-H. Chang, J. Koresh, H. Idriss, J. Catal. 185 (1999) 223.
[24] D. Brinkely, T. Engel, J. Phys. Chem. B 104 (2000) 9836.
[25] A. Furube, T. Asahi, H. Masuhara, H. Yamashita, M. Anpo, J. Phys. Chem. B 103 (1999) 3120.
[26] M.A. Henderson, W.S. Epling, C.L. Perkins, C.H.F. Peden, U. Diebold, J. Phys. Chem. 103 (1999) 5328.
[27] H. Yamashita, Y. Ichihashi, M. Harada, G. Stewart, M.A. Fox, J. Catal. 158 (1996) 97.
[28] K.E. Karakitsu, X.E. Verykios, J. Phys. Chem. 97 (1993) 1184.
[29] W.-X. Xu, Z. Shu, J. Zhou, X.-C. Fu, X.-N. Zhao, J. Chem. Soc. Farad. Trans. 93 (1997) 4187.
[30] A. Hengelin, Chem. Rev. 89 (1989) 1861, and references therein.
[31] M. Grätzel, Heterogenous Photochemical Electron Transfer, CRC Press, Boca Raton, FL, 1988.
[32] R.F. Howe, M. Grätzel, J. Phys. Chem. 89 (1985) 4495.
[33] W. Mönch, Semiconductor Surfaces and Interfaces, in: G. Ertl (Ed.), Springer Series in Surface Sciences, Heidelberg, Berlin, 1995.
[34] W.J. Albery, P.N. Bartlett, J. Electrochem. Soc. 131 (1984) 315.
[35] Handbook of Physics and Chemistry, 78th ed., CRC Press, Boca Raton, FL, 1995.
[36] H. Idriss, P. Legaré, G. Maire, Surf. Sci. 515 (2002) 413.